

Electronic Supplementary Information

An electrocatalytic hydrogen production activity with a copper(II) complex supported by dipyridylamine ligand in acidic water

*Nilankar Diyali[†], Meena Chettri[†], Subhajit Saha[†], Ankita Saha[†], Subhankar Kundu[†] Debasis
Mondal[‡], Debasish Dhak[‡] and Bhaskar Biswas^{*, †}*

[†]*Department of Chemistry, University of North Bengal, Darjeeling-734013, India.*

[‡]*Department of Chemistry, Sidho-Kanho-Birsha University Purulia, 732104, India.*

Table of Content

		Page No.
A.	Experimental	S1- S2
	1. Physical measurements	S1
	2. HER by $[\text{Cu}(\text{dpa})_2(\text{N}_3)]^+$	S1
	3. Catalyst concentration dependence study	S1- S2
	4. DFT Study	S2
B.	Figures	S3-S12
	1. FT-IR spectra of $[\text{Cu}(\text{dpa})_2(\text{N}_3)]^+$	S3
	2. (a) UV-Vis spectra of $[\text{Cu}(\text{dpa})_2(\text{N}_3)]^+$ in water; (b) UV-Vis spectra of $[\text{Cu}(\text{dpa})_2(\text{N}_3)]^+$ in water for stability test over 3 days; (c) UV-Vis spectra of $[\text{Cu}(\text{dpa})_2(\text{N}_3)]^+$ and in presence of 0.1 M KCl in water media.	S3
	3. ESI-MS of $[\text{Cu}(\text{dpa})_2(\text{N}_3)]^+$ in water	S3
	4. Structural validity of the $[\text{Cu}(\text{dpa})_2(\text{N}_3)]\text{Cl}\cdot 4\text{H}_2\text{O}$ with crystallographic bond distance and bond angle measurement.	S4
	5. CVs of GCE , dpa and $[\text{Cu}(\text{dpa})_2(\text{N}_3)]^+$	S4
	6. Plot of current vs. scan rate of $[\text{Cu}(\text{dpa})_2(\text{N}_3)]^+$.	S5
	7. Comparison of the CV of $\text{CuCl}_2\cdot 2\text{H}_2\text{O}$ salt and $[\text{Cu}(\text{dpa})_2(\text{N}_3)]^+$ with the addition of 14 mM AcOH.	S5
	8. (a) dpa titration with AcOH in 0.1 M KCl; (b) only 0.1 M KCl titration with AcOH	S6
	9. (a) CVs in 0.1 M KCl solution in the presence of 14 mM AcOH (red) and with $[\text{Cu}(\text{dpa})_2(\text{N}_3)]^+$ in 14 mM AcOH. (b) CVs were recorded in an electrolyte-only solution using a freshly polished GCE and an electrode after CPE in a solution of 1mM $[\text{Cu}(\text{dpa})_2(\text{N}_3)]^+$ and 14 mM AcOH for 3 h.	S6
	10. Plot of catalytic current (i_c) vs. concentration of AcOH.	S7
	11. CVs in 0.1 M KCl aqueous solution containing 14 mM AcOH with different concentrations of $[\text{Cu}(\text{dpa})_2(\text{N}_3)]^+$ at a scan rate of 100 mV/s.	S7
	12. Hydrogen gas detection by gas chromatography (GC).	S8
	13. CV of complex and recovered complex.	S8
	14. UV-Vis titration of $[\text{Cu}(\text{dpa})_2(\text{N}_3)]^+$ using 0.5 to 11 mM of AcOH.	S9
	15. (a) UV-Vis plot of $[\text{Cu}(\text{dpa})_2(\text{N}_3)]^+$ in a citrate-phosphate buffer in the pH range of 3-7. (b) Plot of absorbance vs. pH at 345 nm.	S9

16.	UV-Vis titration of dpa using 0.5 to 11 mM of AcOH.	S10
17.	Decrement of the d-d band of the $[\text{Cu}(\text{dpa})_2(\text{N}_3)]^+$.	S10
18.	Energy profile of different N-protonated species using DFT calculation.	S11
19.	UV-Vis spectra of $[\text{Cu}(\text{dpa})_2(\text{N}_3)]^+$ in water and after one equivalent sodium naphthalene as one electron reductant.	S11
20.	The spin density plot of N-site protonated.	S12
21.	Optimized structure of intermediates.	S12
C.	Calculation	S13- S14
1.	Determination of diffusion coefficient (D) of $[\text{Cu}(\text{dpa})_2(\text{N}_3)]^+$ in 0.1 M KCl aqueous solution	S13
2.	Calculation of net charge based on Control potential Electrolysis (CPE) in aqueous	S13
3.	Calculation of theoretical Moles of Hydrogen Made via Total Charge	S13
4.	Calculation of Turnover number (TON)	S14
D.	Tables	S15-S31
1.	Crystallographic structural parameters of $[\text{Cu}(\text{dpa})_2(\text{N}_3)]\text{Cl}\cdot 4\text{H}_2\text{O}$	S15
2.	Selected bond distances (Å) and angles (°) of $[\text{Cu}(\text{dpa})_2(\text{N}_3)]\text{Cl}\cdot 4\text{H}_2\text{O}$	S16
3.	Hydrogen bond lengths (Å) and angles (°) for $[\text{Cu}(\text{dpa})_2(\text{N}_3)]\text{Cl}\cdot 4\text{H}_2\text{O}$	S16
4.	X $\cdots\pi$ bond lengths (Å) and angles (°) for $[\text{Cu}(\text{dpa})_2(\text{N}_3)]\text{Cl}\cdot 4\text{H}_2\text{O}$	S17
5.	Electrochemical experimental results from a typical AcOH titration of $[\text{Cu}(\text{dpa})_2(\text{N}_3)]^+$	S17
6.	Approximate catalytic rate constants, k_{app} , with AcOH.	S17
7.	Comparison of homogeneous HER activity with reported Copper complexes.	S18
8.	Computational coordinates using B3LYP/6-311g(d,p) in water.	S18-S31
F.	References	S32

A. Experimental

Physical measurements

FT-IR spectra of $[\text{Cu}(\text{dpa})_2(\text{N}_3)]\text{Cl}\cdot 4\text{H}_2\text{O}$ were recorded using an FTIR-8400S SHIMADZU spectrometer in the $400\text{-}3600\text{ cm}^{-1}$ range. Steady-state absorption spectral data of $[\text{Cu}(\text{dpa})_2(\text{N}_3)]\text{Cl}\cdot 4\text{H}_2\text{O}$ was measured with a HITACHI U-2910 spectrophotometer. A Perkin Elmer 2400 CHN microanalyzer was employed to carry out the elemental analyses of the compounds. The structural characteristics of $[\text{Cu}(\text{dpa})_2(\text{N}_3)]\text{Cl}\cdot 4\text{H}_2\text{O}$ were determined by powder X-ray diffractometer (Rigaku SmartLab) using Cu-K_α radiation ranging from $10^\circ\text{-}80^\circ$. An RVL PG-Lyte-1.0 potentiostat consisting of a glassy-carbon working electrode, Pt counter electrode, and Ag/AgCl reference was employed to study the electrochemical analysis of the compounds.

HER by $[\text{Cu}(\text{dpa})_2(\text{N}_3)]^+$

To investigate the hydrogen evolution activity, CV was recorded by taking 11.1 mg (1 mM) of $[\text{Cu}(\text{dpa})_2(\text{N}_3)]^+$ in 0.1 M KCl, a supporting electrolyte in 20 ml aqueous solution. The 1 M acetic acid (AcOH) in a 10 ml volumetric flask was prepared as a stock solution to monitor the acid titration. The subsequent CVs were recorded with the addition of AcOH from the 0.1 M stock solution in the following amounts of 100 μL , 200 μL , 300 μL , 400 μL and so on. The pH of the solution of 1 mM $[\text{Cu}(\text{dpa})_2(\text{N}_3)]^+$ in 0.1 M KCl was 6.20, recorded using Eutech pH 700 meter. In the same solution, with the addition of 14 mM AcOH and 18 mM AcOH, the pH was 3.56 and 3.17, respectively.

Catalyst concentration dependence study

A 0.1 M stock solution of $[\text{Cu}(\text{dpa})_2(\text{N}_3)]^+$ was prepared by dissolving 0.555 g $[\text{Cu}(\text{dpa})_2(\text{N}_3)]\text{Cl}\cdot 4\text{H}_2\text{O}$ crystals with H_2O in a 10 mL volumetric flask. A 20 mL solution of 0.1 M KCl in H_2O was prepared in an electrochemical cell. 14 mM AcOH was added to the cell and

purged with nitrogen. CVs were taken from 0.0 to -1.6 V at 100 mV/s with the addition of 50 μL , 100 μL , 150 μL , 200 μL , and 250 μL of the $[\text{Cu}(\text{dpa})_2(\text{N}_3)]^+$ stock solution.

DFT study

All the structures were optimized by Density functional theory (DFT) by using the B3LYP functional¹ and 6-311g(d,p) basic set. The calculation in water ($\epsilon = 78.3553$) medium using IEFPCM solvation methods. Gauss view was used as a visualization tool, and all the analysis was carried out by Gaussian 16.² After obtaining the converged geometry, the vibrational harmonic frequencies were calculated at the same theoretical level to ensure that the imaginary frequency number was zero for the stationary point.

B. Figures

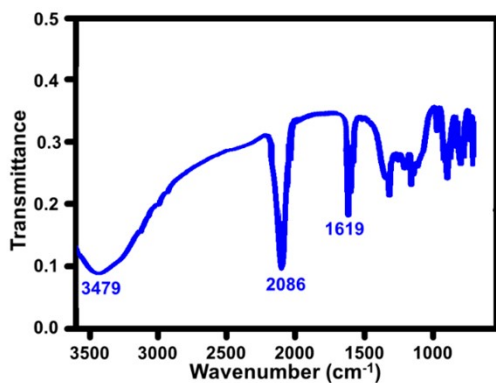


Figure S1. FT-IR spectra of [Cu(dpa)₂(N₃)]Cl·4H₂O.

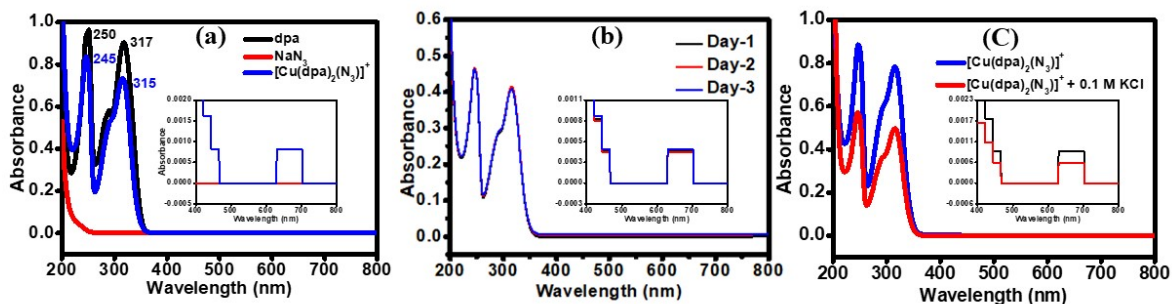


Figure S2. (a) UV-Vis spectra of [Cu(dpa)₂(N₃)]⁺ in water; (b) UV-Vis spectra of [Cu(dpa)₂(N₃)]⁺ in water for stability test over 3 days; (c) UV-Vis spectra of [Cu(dpa)₂(N₃)]⁺ in water and the presence of 0.1 M KCl in water media.

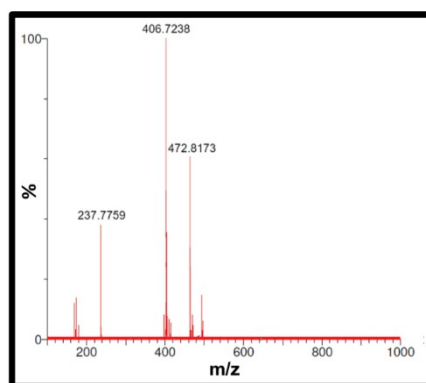


Figure S3. ESI-MS of [Cu(dpa)₂(N₃)]⁺ in water.

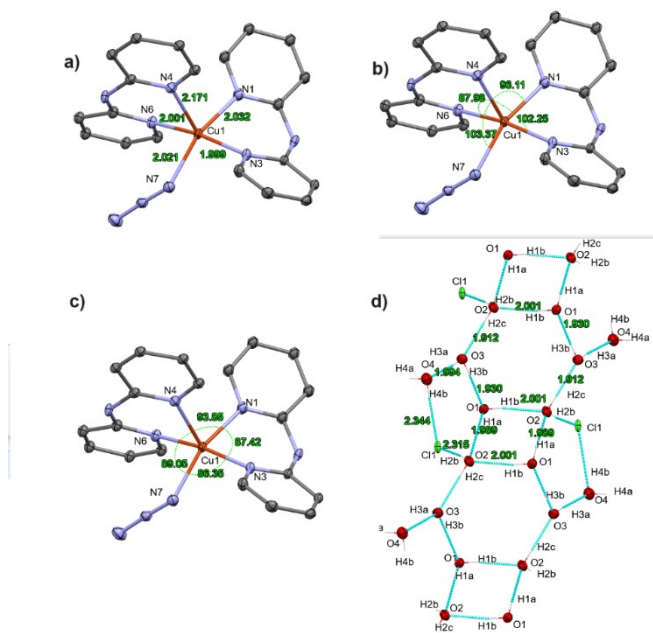


Figure S4. Structural validity of the copper complex with crystallographic bond distance and bond angle measurement.

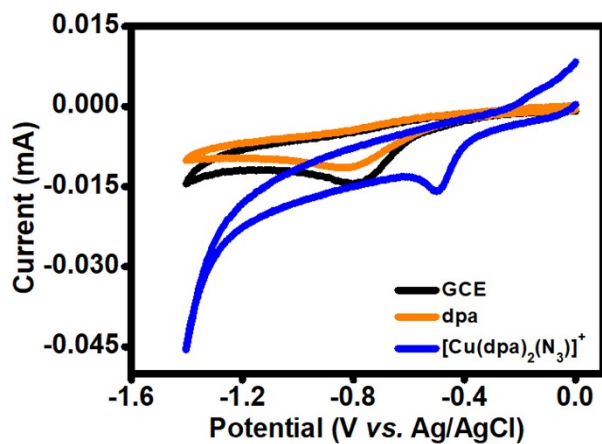


Figure S5. CVs of GCE (black), dpa (orange), and (blue) $[\text{Cu}(\text{dpa})_2(\text{N}_3)]^+$. Peak around -0.8 V vs. Ag/AgCl is due to dissolved O_2 .

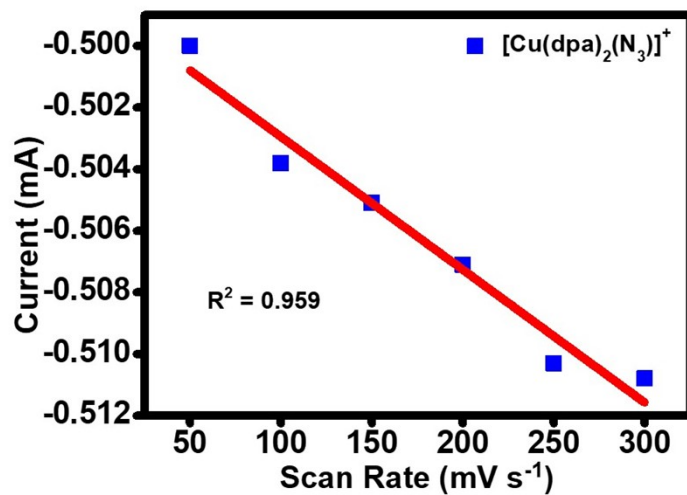


Figure S6. Plot of current vs. scan rate of $[\text{Cu}(\text{dpa})_2(\text{N}_3)]^+$.

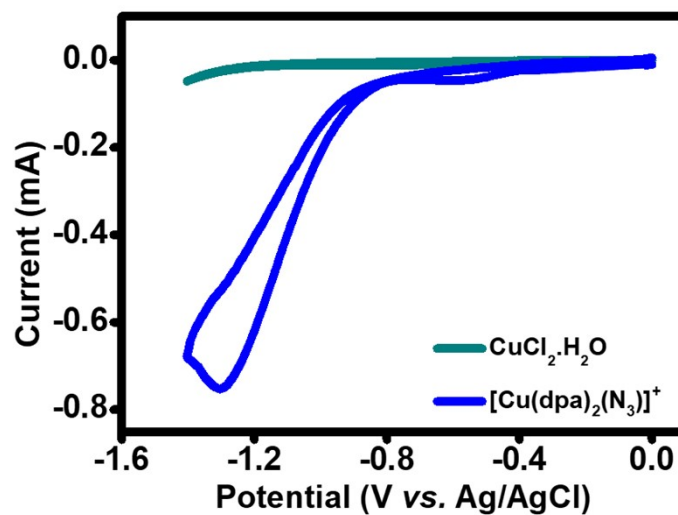


Figure S7. Comparison of CV of $\text{CuCl}_2 \cdot 2\text{H}_2\text{O}$ salt and $[\text{Cu}(\text{dpa})_2(\text{N}_3)]^+$ with addition of 14 mM AcOH.

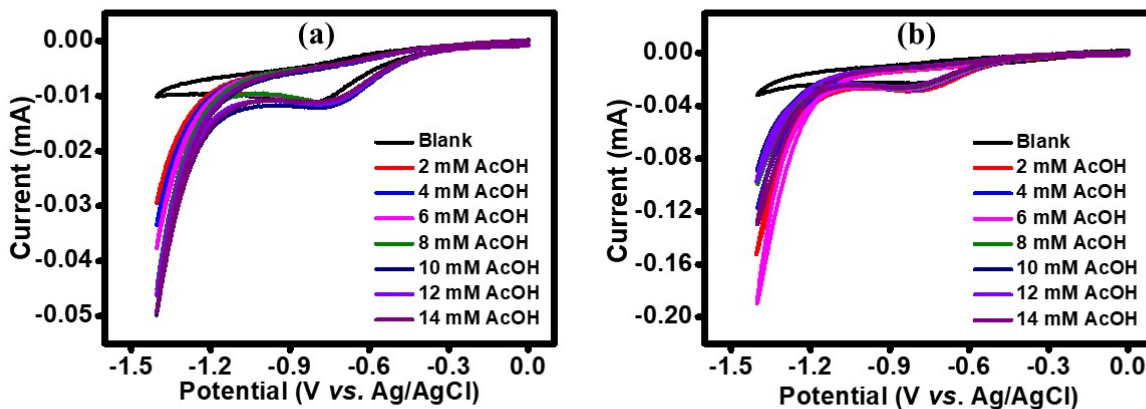


Figure S8. (a) dpa titration with AcOH in 0.1 M KCl; (b) only 0.1 M KCl titration with AcOH. (the appearance of a peak at around -0.8V (V vs. Ag/AgCl) is due to the presence of oxygen.)

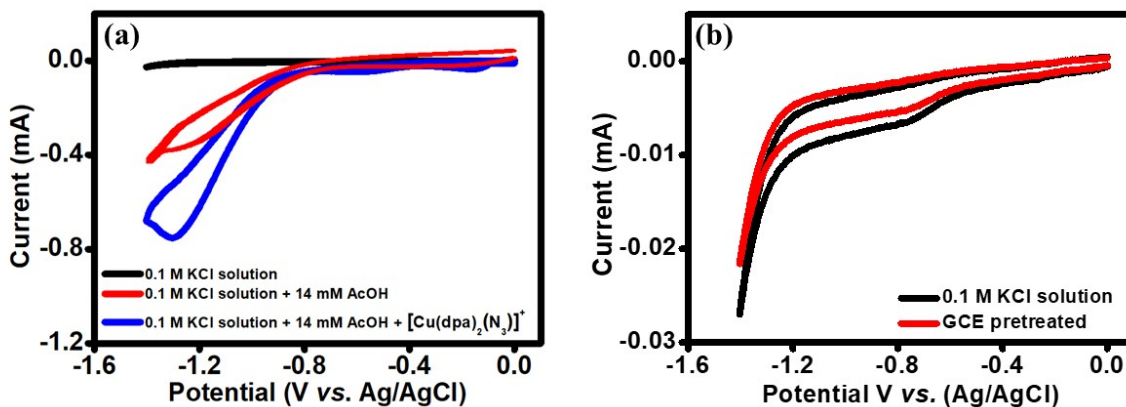


Figure S9. (a). CVs run in 0.1 M KCl as an electrolyte in aqueous solution (black), in the presence of 14 mM AcOH (red) and the presence of $[\text{Cu}(\text{dpa})_2(\text{N}_3)]^+$ with 14 mM AcOH (blue). (b) CVs were recorded in an electrolyte-only solution using a freshly polished GCE (black trace) and an electrode after CPE in a solution of 1mM $[\text{Cu}(\text{dpa})_2(\text{N}_3)]^+$ and 14 mM AcOH for 3 h (red trace).

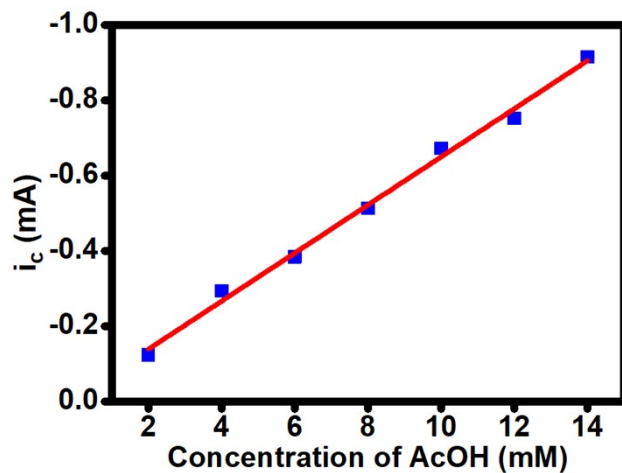


Figure S10. Plot of catalytic current (i_c) vs. concentration of AcOH.

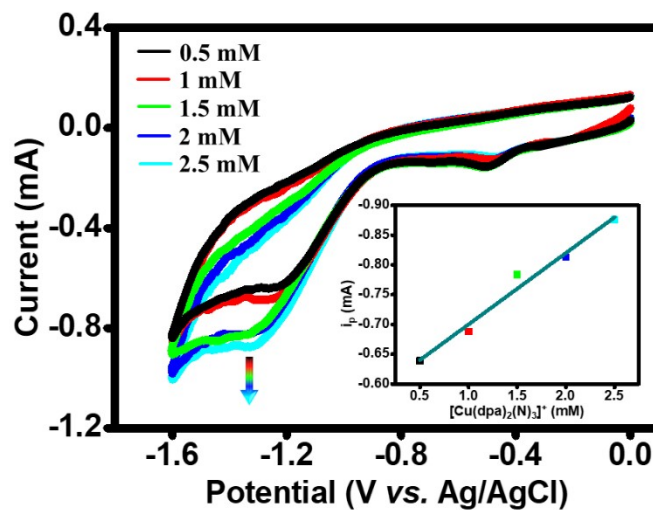


Figure S11. CVs in 0.1 M KCl aqueous solution containing 14 mM AcOH with different concentrations of $[\text{Cu}(\text{dpa})_2(\text{N}_3)]^+$ at a scan rate of 100 mV/s. Inset i_p vs. $[\text{Cu}(\text{dpa})_2(\text{N}_3)]^+$ fitted with a linear correlation exhibiting an R^2 value of 0.99.

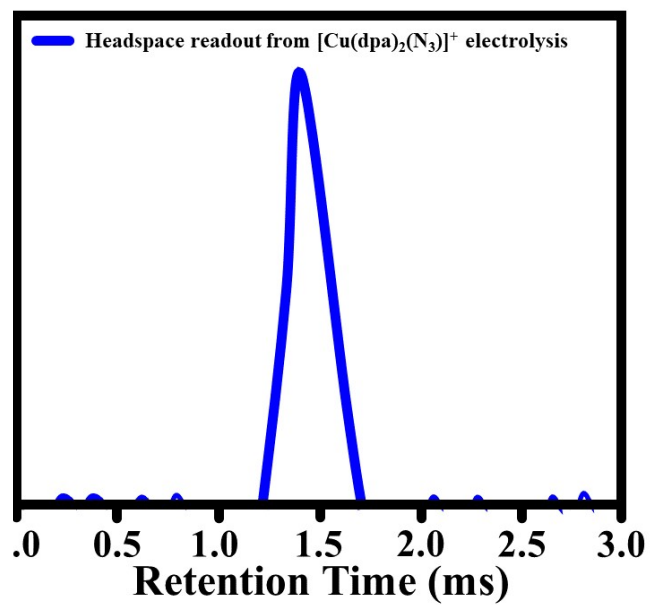


Figure S12. Hydrogen gas detection by gas chromatography (GC).

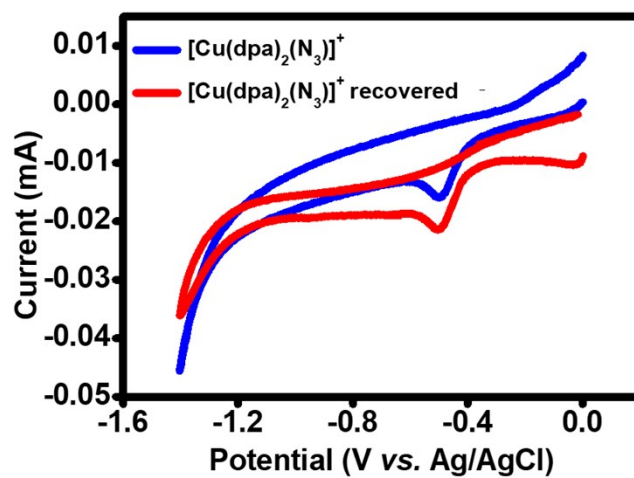


Figure S13. CV of complex and recovered complex.

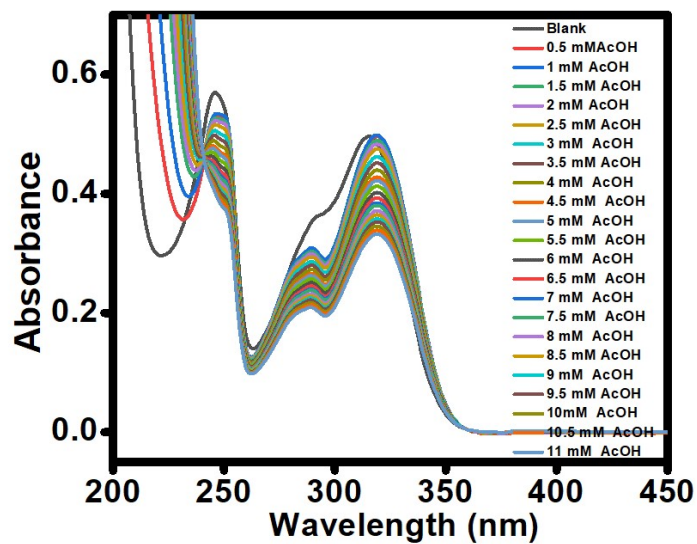


Figure S14. UV-Vis titration of $[\text{Cu}(\text{dpa})_2(\text{N}_3)]^+$ using 0.5 to 11 mM of AcOH.

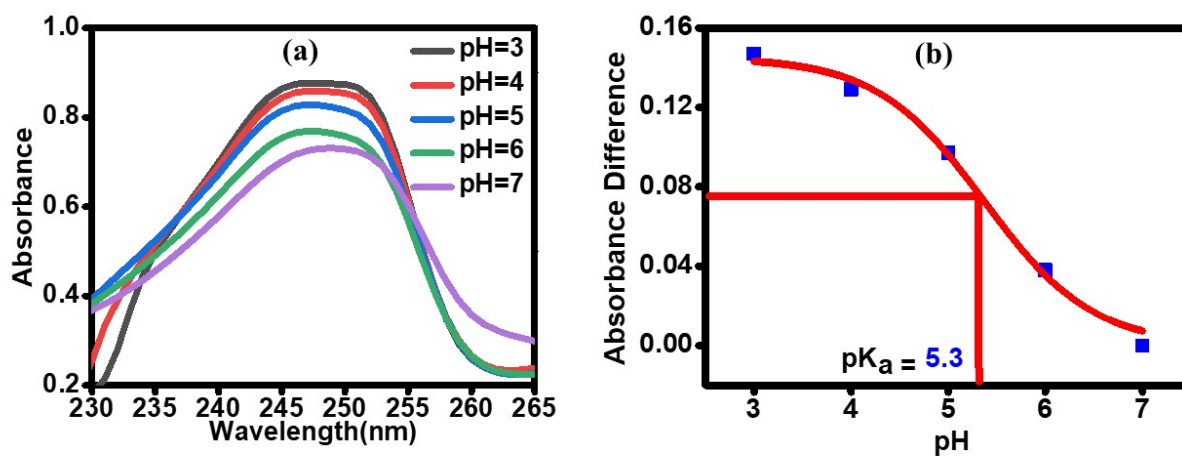


Figure S15. (a) UV-Vis plot of $[\text{Cu}(\text{dpa})_2(\text{N}_3)]^+$ in a citrate-phosphate buffer in the pH range of 3-7. (b) Plot of absorbance vs. pH at 345 nm.

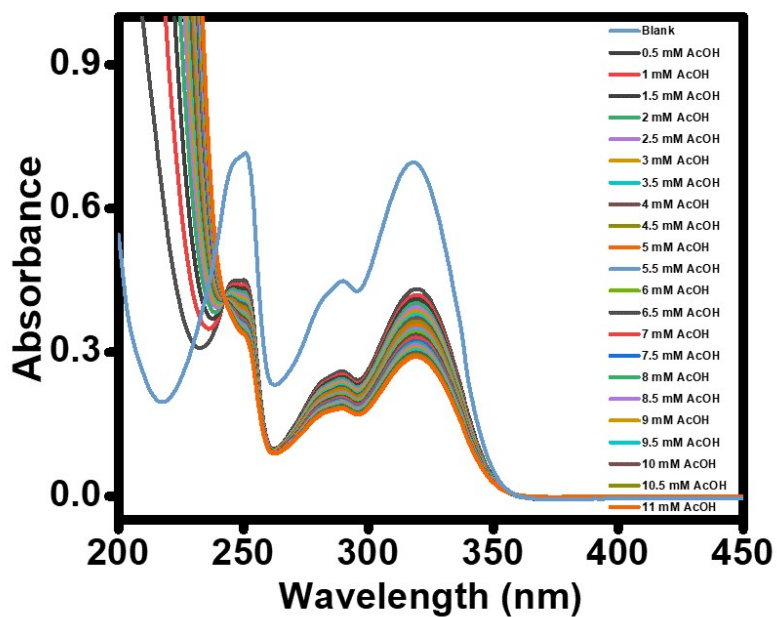


Figure S16. UV-Vis titration of dpa using 0.5 to 11 mM of AcOH.

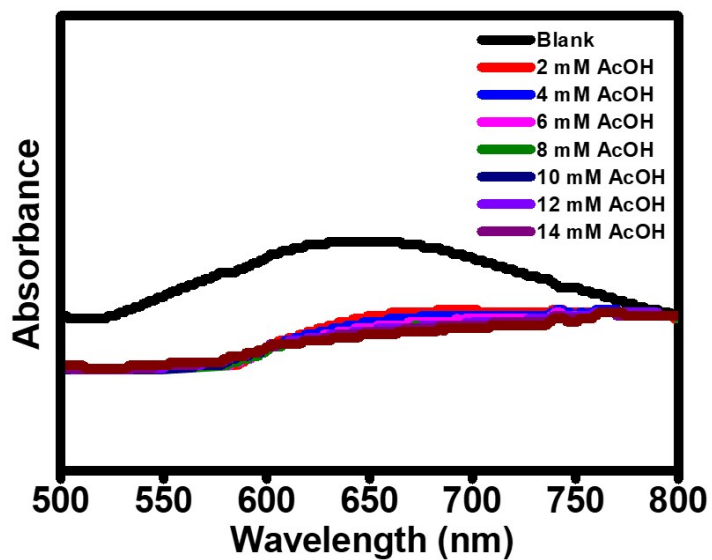


Figure S17. Decrement of the d-d band of the $[\text{Cu}(\text{dpa})_2(\text{N}_3)]^+$. A high concentration of complex was used to clarify the d-d band.

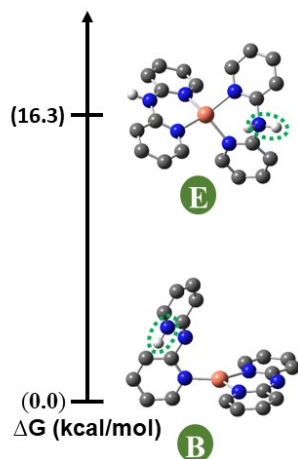


Figure S18. Energy profile of different N-protonated species using DFT calculation.

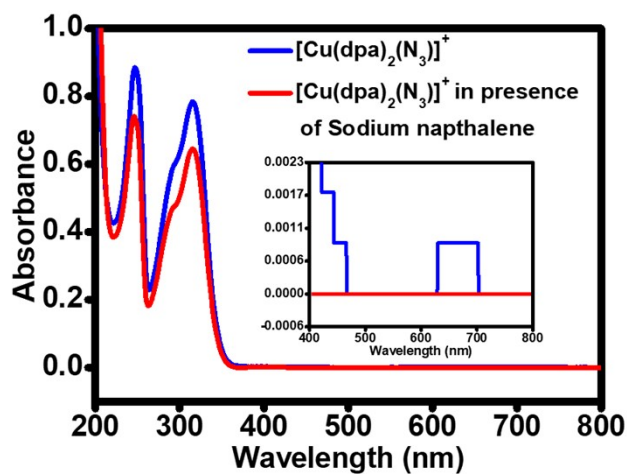


Figure S19. UV-Vis spectra of $[\text{Cu}(\text{dpa})_2(\text{N}_3)]^+$ in water (blue) and after one equivalent sodium naphthalene as one electron reductant (red). Inset: Diminishing nature of d-d band.

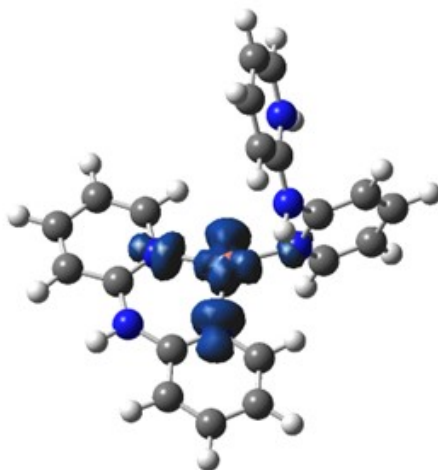


Figure S20. The spin density plot of N-site protonated intermediate (B) at an isovalue of 0.003.

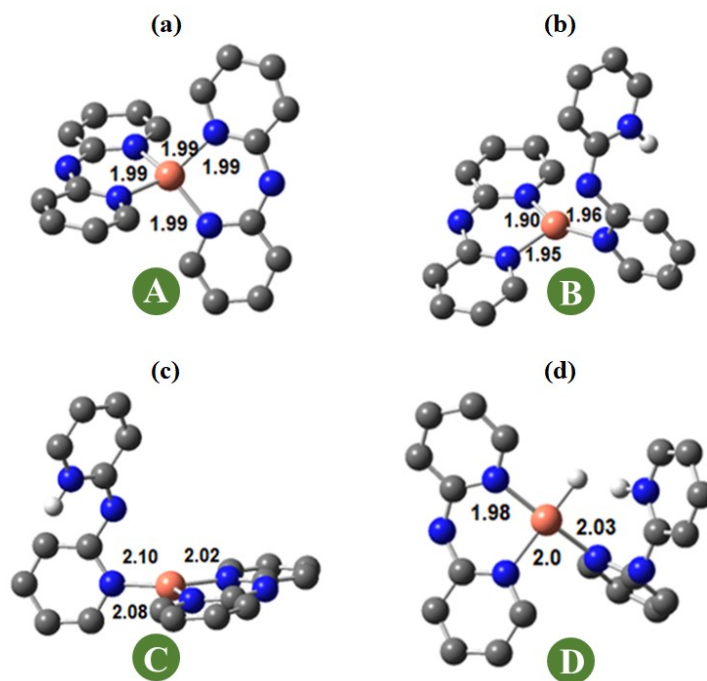


Figure S21: Optimized structure of intermediates a) N-site protonation of Cu(II) state, b) N-site protonation of Cu(I) state, c) doubly protonated Cu(II) intermediate state in Tafel step of $[\text{Cu}(\text{dpa})_2(\text{N}_3)]^+$ electrocatalyst.

C.CALCULATION

1. Determination of the diffusion coefficient (D) of [Cu(dpa)₂(N₃)]⁺ in 0.1 M KCl aqueous solution

The Diffusion Coefficient (D) was extracted from the theoretical slope using the equation below-

$$Slope = [0.4463nFAC^0 \left(\frac{nFD}{RT}\right)^{\frac{1}{2}}] \dots\dots\dots(S1)$$

$$D = \left(\frac{slope}{0.4463 n F A C^0}\right)^2 \frac{RT}{nF} \dots\dots\dots(S2)$$

Slope ≡ 3.65 × 10⁻³

Area of the glassy carbon electrode (A) = 0.071 cm²

Concentration of the analyte (C) = 1 × 10⁻³ moles/cm

Faraday constant (F) = 96485 C/mole e⁻

R = ideal gas constant, and T = 298 K

$$D_0 = 4.432 \times 10^{-3} \text{ cm}^2 / \text{s}$$

2. Calculations of net charge based on Control potential Electrolysis (CPE) in aqueous 0.1 M KCl:

Total charge = Q_{with cat} - Q_{blank} = Q_{net}

= 8.143 C - 0.04568 C = 8.09732 C

3. Calculation of theoretical Moles of Hydrogen Made via Total Charge

Moles H₂ theoretical = 8.143 x (1 mol e⁻ / 96485 C) x (1 mol H₂ / 2 mol e⁻)

= 4.196 × 10⁻⁵ moles H₂ based on the charge from electrolysis

4. Calculation of turnover number (TON)

$$TON = \frac{\text{Moles of } H_2 \text{ produced}}{\text{Moles of } [Cu(dpa)_2(N_3)]^+ \text{ used}}$$

$$\text{TON} = \frac{4.196 \times 10^{-5} \text{ moles } H_2 \text{ produced}}{0.000001 \text{ moles } [Cu(dpa)_2(N_3)]^+ \text{ used}}$$

$$\text{TON} = 41.96$$

Assuming two electrons are passed for each H₂ molecule produced (n=2), and the acid concentration does not change significantly during the measurement, the catalytic turnover frequency (k_{obs} = k[H⁺]) can be calculated using equation

$$\frac{i_{cat}}{i_p} = \frac{n}{0.4463} \sqrt{\frac{RT(K [H^+])}{Fv}} \dots\dots\dots(S3)$$

The apparent rate constant (k_{app}) associated with acid and catalyst is calculated using the **equation S4**.

$$i_c = nFAC_{cat}(Dk_{app}C_{acid})^{1/2} \dots\dots\dots(S4)$$

D. Tables

Table S1. Crystallographic structural parameters of [Cu(dpa)₂(N₃)]Cl·4H₂O	
Parameters	[Cu(dpa)₂(N₃)]Cl·4H₂O
CCDC	2299272
Empirical formula	C ₂₀ H ₂₆ ClCuN ₉ O ₄
Formula weight	555.49
T (K)	250K
Wavelength (Å)	1.54184
Crystal system	Monoclinic
Space group	<i>P21/c</i>
Unit Cell Dimensions	
a (Å)	7.0295(4)
b (Å)	27.8164(16)
c (Å)	12.8722(7)
α (°)	90.00
β (°)	99.071(5)
γ (°)	90
V (Å ³)	2485.5(2)
Z	4
ρ (g cm ⁻³)	1.485
Absorption coefficient (mm ⁻¹)	1.032
F(000)	1148
Theta range for data collection	2.7 to 32.8
Index ranges (h, k, l)	-8 ≤ h ≤ 8, -29 ≤ k ≤ 30, -14 ≤ l ≤ 9
Reflections collected	16212
Independent reflections	4195

R(int)	0.021
Final R indices [I>2sigma(I)]	R ₁ = 0.0605, wR ₂ = 0.1593
Largest diff. peak and hole	1.45/-1.13 e. Å ⁻³

Table S2. Selected bond distances (Å) and angles (°) of [Cu(dpa)₂(N₃)]Cl·4H₂O.					
	Exp.	DFT		Exp.	DFT
Cu1-N3	1.999(3)	2.0692	Cu1-N8	2.033(3)	2.0783
Cu1-N4	2.170(3)	2.2837	Cu1-NC	2.021(3)	1.9547
Cu1-N5	2.001(3)	2.0624			
∠N3-Cu1-N4	102.27(10)	107.02	∠N3-Cu1-NC	86.33(11)	87.38
∠N3-Cu1-N5	169.51(11)	167.73	∠N4-Cu1-N5	87.97(10)	85.23
∠N3-Cu1-N8	87.40(11)	86.52	∠N4-Cu1-N8	96.15(11)	94.29
∠N4-Cu1-NC	103.38(11)	97.29	∠N5-Cu1-NC	89.09(11)	90.82
∠N5-Cu1-N8	93.84(11)	92.95	∠N8-Cu1-NC	160.34(11)	168.06

D–H···A	<i>d</i> (D–H)	<i>d</i> (H···A)	<i>d</i> (D···A)	∠(DHA)	Symmetry
O1--H1B..Cl5	0.85	2.31	3.156(3)	171	x,y,1+z
NA--HA..Cl5	0.86	2.55	3.251(2)	139	x,y,1+z
O2--H2B..Cl5	0.85	2.34	3.193(4)	177	-1+x,y,z
O3--H3A..O4	0.85	1.93	2.781(4)	175	-x,1-y,2-z
O3--H3B..O2	0.85	1.99	2.842(4)	177	x,y,1+z
O4--H4A..O1	0.85	1.99	2.842(4)	177	1-x,1-y,2-z
CN--HN..NC	0.93	2.59	3.464(4)	156	x,3/2-y,1/2+z

X···Cg(<i>I</i>)	<i>d</i> [X···Cg(<i>I</i>)]	∠[CHCg(<i>I</i>)]
N9-NL[1] -> Cg5	3.357(4)	8.76

[[Cu(dpa) ₂ (N ₃)] ⁺ (mM)	AcOH (mM)	<i>i</i> _c (mA)	<i>i</i> _p (mA)	<i>i</i> _{cat} / <i>i</i> _p	Scan rate (ϑ, V/s)	<i>k</i> _{obs} (s ⁻¹)
1	2	-0.124	-0.0569	2.17	0.1	0.90
1	4	-0.2944	-0.0569	5.166	0.1	5.15
1	6	-0.3847	-0.0569	6.75	0.1	8.79
1	8	-0.5132	-0.0569	9.006	0.1	15.65

Table S7. Comparison of homogeneous HER activity with reported Copper complexes.

S. No	Electrocatalyst	TON	Electrochemical media/proton source	Stability/Durability			
1	1	10	-0.6727	11.89	0.1	23.68	
1	12	-0.7517	-0.0569	13.19	0.1	33.56	
1	¹ [(bztpen)Cu](BF ₄) ₂ ³	14	-0.9157 10000 s ⁻¹	-0.0569 Acidic aqueous buffer.	16.07	0.1	49.81 Not explicitly discussed
2	[Cu(TMPA)Cl]Cl (1) and [Cu(Cl-TMPA)Cl ₂] (2) ⁴	(1) 6108 TON and (2) 10014 TON in 6 h	CH ₃ CN/H ₂ O solution (9:1, v/v) with Ir complex as PS and triethylamine (TEA) as sacrificial reductant (SR).	After electrolysis for 2 h, characteristic NIR absorption of Cu(II) species was diminished.			
3	[Cu(QCl-tpy)(OAc)(Cl)] (1), and [Cu(4Ql-tpy)(OAc)(OH ₂)Cl] (2) ⁵	(1) 1153 s ⁻¹ (2) 1682 s ⁻¹	95:5 DMF/H ₂ O (v/v) in the presence of AcOH as a proton source.	Not explicitly discussed			
4	[Cu(tpen)](PF ₆) ⁶	3415 s ⁻¹	95:5 DMF/H ₂ O (v/v) in the presence of AcOH as a proton source.	1)After electrolysis for 2 h, some minor spectral changes were observed in the UV–vis spectra. 2)FESEM and EDX analyses revealed a slight decomposition of copper on working electrode.			

Table S6. Approximate catalytic rate constants, *k*_{app}, with AcOH, were obtained using equation S4.

<i>k</i> _{app} (2 mM) M ⁻¹ s ⁻¹	<i>k</i> _{app} (4 mM) M ⁻¹ s ⁻¹	<i>k</i> _{app} (6 mM) M ⁻¹ s ⁻¹	<i>k</i> _{app} (8 mM) M ⁻¹ s ⁻¹	<i>k</i> _{app} (10 mM) M ⁻¹ s ⁻¹	<i>k</i> _{app} (12mM) M ⁻¹ s ⁻¹	<i>k</i> _{app} (14mM) M ⁻¹ s ⁻¹
9.214	26.04	29.64	39.56	54.39	56.59	71.99

5	$[\{(\text{OAc})_2\text{Cu}(\text{3py-tpy})\}_2\text{Cu}(\text{OAc})_2(\text{H}_2\text{O})_2]$ (1), $\{[\text{Cu}(\text{4pytpy})(\text{OAc})]\text{Cl}\}_n$ (2) and $[\text{Cu}(\text{Ph-tpy})(\text{OAc})_2]$ (3) ⁷	(1) 1473 s ⁻¹ (2) 700 s ⁻¹ (3) 926 s ⁻¹	95:5 DMF/H ₂ O (v/v) in the presence of AcOH as a proton source.	No substantial change in the CV and UV-vis spectrum recorded before and after the bulk electrolysis.
6	Cu(II)L , ⁸	10000 s ⁻¹ and TON 52 in ACN and 5100 s ⁻¹ and TON 73 in DMF	ACN and DMF with AcOH as a proton source.	CPE reveals no sign of degradation over 23 h.
7	[Cu(dpa)₂(N₃)]⁺ This work	241.75 s ⁻¹ and TON 73.06	AcOH in 0.1 M KCl water.	CPE reveals no sign of degradation over 1.6 h, PXRD, UV-vis spectrum displays negligible change after electrolysis.

Table S8. Computational coordinates using B3LYP/6-311g(d,p) in water.

[Cu(dpa)₂(N₃)]⁺			
Cu	0.15354	-0.04865	-0.43176
N	2.04503	-0.8642	-0.62854
N	0.8458	-1.09566	1.33476
N	-1.61447	1.00169	-0.58804
N	-2.97803	-0.69098	0.39302
H	-3.92057	-1.04878	0.36296
N	1.04564	1.41737	0.74062
N	3.11906	1.23032	-0.37668
H	3.99588	1.70485	-0.53196

C	3.16034	-0.12685	-0.70001
C	-2.1384	-1.41543	1.23658
C	-2.82717	0.48993	-0.31667
C	-2.70956	-2.46581	1.97881
H	-3.76068	-2.7061	1.8699
C	2.281	1.88954	0.51131
C	4.38883	-0.67407	-1.10142
H	5.26937	-0.04575	-1.16212
C	-0.08507	-1.78824	2.2028
H	0.95486	-1.48409	2.25464
C	4.45422	-2.02167	-1.39913
H	5.39435	-2.46346	-1.70688
C	-1.5469	2.15954	-1.28671
H	-0.54808	2.53494	-1.47407
C	0.28786	2.03921	1.67228
H	-0.68297	1.59575	1.84264

C	-4.00322	1.1301	-0.75693
H	-4.96751	0.69424	-0.52591
C	2.1245	-2.18165	-0.91836
H	1.18418	-2.71402	-0.88899
C	-1.90783	-3.17518	2.85137
H	-2.32734	-3.98734	3.4329
C	3.30037	-2.80063	-1.2911
H	3.30834	-3.85879	-1.51436
C	-0.55957	-2.82734	2.98033
H	0.09853	-3.35285	3.65923
C	-2.65041	2.83982	-1.74836
H	-2.53279	3.75643	-2.31003
C	2.76243	3.04717	1.15017
H	3.75928	3.41042	0.93071
C	-3.91306	2.29917	-1.47872
H	-4.81224	2.79225	-1.82743
C	0.69701	3.16125	2.36039

H	0.04643	3.6183	3.09352
C	1.96088	3.68738	2.0724
H	2.31955	4.57525	2.57911

E			
Cu	-0.00001	-0.00013	0.00004
N	1.36091	1.27771	0.69414
N	-1.36029	1.27841	-0.69394
N	-1.36113	-1.27792	0.6938
N	-3.23793	0.00044	-0.00082
H	-3.84142	0.43446	0.66808
N	-1.36055	-1.27875	-0.6934
H	4.2481	-0.0004	-0.00054
C	2.68775	1.06124	0.68852

C	2.68719	1.06219	-0.68901
C	-2.68794	-1.06122	0.6881
C	-3.56984	1.92165	-1.37146
H	-4.63398	1.72683	-1.34043
C	2.68737	-1.06215	-0.6886
C	3.57089	1.92035	1.37078
H	4.63499	1.72534	1.33917
C	-0.87579	2.33051	-1.40445
H	0.1989	2.44856	-1.39645
C	3.06395	2.99009	2.0737
H	3.73463	3.65515	2.60316
C	-0.87736	-2.32983	1.40505
H	0.1973	-2.44824	1.39769
C	0.87625	-2.33085	-1.40402
H	-0.1984	-2.44922	-1.39584
C	-3.57125	-1.92008	1.37046

H	-4.6353	-1.72485	1.33884
C	0.87693	2.32965	1.40524
H	-0.19774	2.44791	1.39777
C	-3.06237	2.99154	-2.07378
H	-3.73267	3.65687	-2.60336
C	1.67987	3.20151	2.10069
H	1.23986	4.02188	2.64997
C	-1.67824	3.20274	-2.1
H	-1.23781	4.02322	-2.64878
C	-1.68047	-3.20149	2.10056
H	-1.24061	-4.02188	2.64995
C	3.57018	-1.9212	-1.37137
H	4.63427	-1.72607	-1.34047
C	-3.06452	-2.98983	2.07351
H	-3.73532	-3.6547	2.60304
C	1.67885	-3.20272	-2.09986

H	1.2386	-4.02323	-2.64874
C	3.06292	-2.99108	-2.07385
H	3.73332	-3.65609	-2.6037
H	-3.84045	-0.43368	-0.67053
B			
Cu	-0.00001	-0.00013	0.00004
N	1.36091	1.27771	0.69414
N	-1.36029	1.27841	-0.69394
N	-1.36113	-1.27792	0.6938
N	-3.23793	0.00044	-0.00082
H	-4.2481	0.0006	-0.0011
N	1.36055	-1.27875	-0.6934
N	3.23794	-0.00047	-0.00016
H	4.2481	-0.0004	-0.00054
C	2.68775	1.06124	0.68852
C	-2.68719	1.06219	-0.68901
C	-2.68794	-1.06122	0.6881

C	-3.56984	1.92165	-1.37146
H	-4.63398	1.72683	-1.34043
C	2.68737	-1.06215	-0.6886
C	3.57089	1.92035	1.37078
H	4.63499	1.72534	1.33917
C	-0.87579	2.33051	-1.40445
H	0.1989	2.44856	-1.39645
C	3.06395	2.99009	2.0737
H	3.73463	3.65515	2.60316
C	-0.87736	-2.32983	1.40505
H	0.1973	-2.44824	1.39769
C	0.87625	-2.33085	-1.40402
H	-0.1984	-2.44922	-1.39584
C	-3.57125	-1.92008	1.37046
H	-4.6353	-1.72485	1.33884
C	0.87693	2.32965	1.40524

H	-0.19774	2.44791	1.39777
C	-3.06237	2.99154	-2.07378
H	-3.73267	3.65687	-2.60336
C	1.67987	3.20151	2.10069
H	1.23986	4.02188	2.64997
C	-1.67824	3.20274	-2.1
H	-1.23781	4.02322	-2.64878
C	-1.68047	-3.20149	2.10056
H	-1.24061	-4.02188	2.64995
C	3.57018	-1.9212	-1.37137
H	4.63427	-1.72607	-1.34047
C	-3.06452	-2.98983	2.07351
H	-3.73532	-3.6547	2.60304
C	1.67885	-3.20272	-2.09986
H	1.2386	-4.02323	-2.64874
C	3.06292	-2.99108	-2.07385
H	3.73332	-3.65609	-2.6037
H	-0.74308	0.67785	-0.18563

C			
Cu	-0.66152	-0.27456	-0.63694
N	-1.57501	1.37782	-0.89961
N	3.59672	0.94106	0.11706
N	0.81386	-1.52144	-0.99209
N	1.9313	-0.56059	0.83156
H	1.39113	-0.8833	1.62547
N	-2.02467	-1.08632	0.50166
N	-3.27777	0.92962	0.67801
H	-4.07585	1.33886	1.14356
C	-2.67493	1.76661	-0.2337
C	2.82968	0.43068	1.10839
C	1.9681	-1.42179	-0.29455
C	2.96096	0.97992	2.39268
H	2.35847	0.58348	3.19826
C	-3.07276	-0.39786	0.9917
C	-3.236	3.03714	-0.45472
H	-4.12235	3.33006	0.09246
C	4.49578	1.94549	0.3084
H	5.04871	2.24964	-0.56775
C	-2.65037	3.88074	-1.37228
H	-3.07694	4.85956	-1.55126
C	0.75616	-2.36649	-2.04373

H	-0.19044	-2.43318	-2.56357
C	-1.87792	-2.39656	0.83017
H	-1.02105	-2.90046	0.4073
C	3.09817	-2.1481	-0.63752
H	3.99493	-2.06935	-0.03814
C	-1.01	2.21259	-1.81175
H	-0.13564	1.83762	-2.32896
C	3.85838	2.00479	2.60243
H	3.96039	2.42436	3.59515
C	-1.51197	3.46321	-2.07512
H-	1.03092	4.09535	-2.80773
C	4.64725	2.49963	1.54875
H	5.3599	3.29668	1.70055
C	1.85156	-3.10961	-2.45121
H	1.76381	-3.76614	-3.30552
C	-4.0006	-1.01696	1.84976
H	-4.83417	-0.44192	2.23116
C	3.04119	-2.99471	-1.74184
H	3.91134	-3.57343	-2.02378
C	-2.75409	-3.0574	1.65634
H	-2.59292	-4.10094	1.88652
C	-3.839	-2.34361	2.17952
H	-4.55206	-2.82674	2.83539

H	3.49922	0.57482	-0.82437
D			
Cu	-0.00001	-0.00013	0.00004
N	1.36091	1.27771	0.69414
N	-1.36029	1.27841	-0.69394
N	-1.36113	-1.27792	0.6938
N	-3.23793	0.00044	-0.00082
H	-4.2481	0.0006	-0.0011
N	1.36055	-1.27875	-0.6934
N	3.23794	-0.00047	-0.00016
H	4.2481	-0.0004	-0.00054
C	2.68775	1.06124	0.68852
C	-2.68719	1.06219	-0.68901
C	-2.68794	-1.06122	0.6881
C	-3.56984	1.92165	-1.37146
H	-4.63398	1.72683	-1.34043
C	2.68737	-1.06215	-0.6886
C	3.57089	1.92035	1.37078
H	4.63499	1.72534	1.33917
C	-0.87579	2.33051	-1.40445
H	0.1989	2.44856	-1.39645
C	3.06395	2.99009	2.0737

H	3.73463	3.65515	2.60316
C	-0.87736	-2.32983	1.40505
H	0.1973	-2.44824	1.39769
C	0.87625	-2.33085	-1.40402
H	-0.1984	-2.44922	-1.39584
C	-3.57125	-1.92008	1.37046
H	-4.6353	-1.72485	1.33884
C	0.87693	2.32965	1.40524
H	-0.19774	2.44791	1.39777
C	-3.06237	2.99154	-2.07378
H	-3.73267	3.65687	-2.60336
C	1.67987	3.20151	2.10069
H	1.23986	4.02188	2.64997
C	-1.67824	3.20274	-2.1
H	-1.23781	4.02322	-2.64878
C	-1.68047	-3.20149	2.10056
H	-1.24061	-4.02188	2.64995
C	3.57018	-1.9212	-1.37137
H	4.63427	-1.72607	-1.34047
C	-3.06452	-2.98983	2.07351
H	-3.73532	-3.6547	2.60304
C	1.67885	-3.20272	-2.09986
H	1.2386	-4.02323	-2.64874

C	3.06292	-2.99108	-2.07385
H	3.73332	-3.65609	-2.6037
H	-0.74308	0.67785	-0.18563

E. References

- 1 S. Grimme, *J. Comput. Chem.*, 2006, **27**, 1787–1799.
- 2 2016.
- 3 P. Zhang, M. Wang, Y. Yang, T. Yao and L. Sun, *Angew. Chemie - Int. Ed.*, 2014, **53**, 13803–13807.
- 4 J. Wang, C. Li, Q. Zhou, W. Wang, Y. Hou, B. Zhang and X. Wang, *Dalt. Trans.*, 2016, **45**, 5439–5443.
- 5 S. Rai, S. S. Akhter and S. K. Padhi, *Polyhedron*, 2021, **208**, 115425.

- 6 K. Majee, S. Rai, B. Panda and S. K. Padhi, *Electrochim. Acta*, 2020, **354**, 136614.
- 7 S. Rai and S. K. Padhi, *Electrochim. Acta*, 2020, **364**, 137277.
- 8 A. Z. Haddad, S. P. Cronin, M. S. Mashuta, R. M. Buchanan and C. A. Grapperhaus, *Inorg. Chem.*, 2017, **56**, 11254–11265.